

行政院國家科學委員會專題研究計畫 期中進度報告

子計畫一：污泥膠羽結構對精密分離處置程序之影響(2/3)

計畫類別：整合型計畫

計畫編號：NSC92-2214-E-002-019-

執行期間：92年08月01日至93年07月31日

執行單位：國立臺灣大學化學工程學系暨研究所

計畫主持人：李篤中

報告類型：精簡報告

報告附件：國外研究心得報告

出席國際會議研究心得報告及發表論文

處理方式：本計畫可公開查詢

中 華 民 國 93 年 4 月 26 日

行政院國家科學委員會專題研究計畫成果報告

精密固液分離在高科技產業之應用 子計劃一 污泥膠羽對精密分離處置之影響 (2/3)

計畫編號：NSC 92-2214-E-002-019

執行期限：92年8月1日至93年7月31日

主持人：李篤中 教授

計畫參與人員：

執行機構及單位名稱：國立台灣大學化學工程學系

I. 中文摘要

本計畫擬以三年時間，藉由數種表面分析與分子生物學的方法，對污泥膠羽顆粒的內部結構作更進一步的探討與解析，以了解及其對後續消化與固液分離兩種操作間之關係。在第二年的報告中，我們採取病理分析中常用的石蠟固定切片觀察污泥膠羽之截面影像，取得二維結構資訊，並使用共軛焦掃描顯微鏡配合核糖核酸螢光探針，建構污泥膠羽之三維模型與分析其表面特性。在本報告中將比較由兩種技術所得到的結構資訊，同時亦探討在經過物理與化學調理後污泥膠羽結構之變化

關鍵詞：結構、膠羽、調理、石蠟切片、共軛焦雷射掃描顯微鏡、核糖核酸螢光探針、三維模型

Abstract

This report summarized the experimental results of the second year in the three-year-project investigating the internal structure of sludge floc by surface analysis tools and molecular biological techniques. The target is to construct the correlation between the floc structure and the subsequent treatment of sludge. To continue the results of the first-year project, we used the paraffin-embedded slicing to obtain the two-dimensional structure from the sliced image of flocs. Confocal laser scanning microscopy tests with fluorescence *in situ* hybridization of 16S rRNA probes were performed to establish the 3D models of the floc. The variation in surface ruggedness and internal structure of sludge flocs in prior and after conditioning were examined in this report.

Keywords: Structure, flocs, conditioning, slicing, confocal laser scanning microscopy, 16S rRNA probes

II. Introduction (計劃緣由與目的)

Sludge conditioning is required to alter the properties of the floc to improve its dewaterability (Moudgil and Shah, 1986). Cationic polyelectrolyte

flocculation and freezing/thawing have been widely investigated. Polyelectrolyte flocculation enhances the dewaterability of sludge by charge neutralization and polymer bridging, leading to the increase in floc size and decrease in the bound water content (Chu and Lee, 1999). On the other hands, freezing/thawing converts the loose floc structure into a compact form by interfacial dehydration of moving ice fronts. This conversion could lead to considerable improvement on the sludge dewaterability (Chu *et al.*, 1997), reduced the pathogen activity (Chu *et al.*, 1999), and separate the oily components from the solids phase of oily sludge (Jean *et al.*, 1999). However, the detailed information on the change in floc structure after conditioning, however, is still largely lacking. This report considers the effects of cationic polyelectrolyte flocculation and freezing/thawing on the characteristics sludge flocs. Free settling tests, small-angle light scattering tests, microtome slicing, confocal laser scanning microscopy were performed to determine the geometric parameters. The fractal dimensions determined from different tests were compared to reveal possible correlations among these parameters.

III. Experimental (實驗方法)

Samples and conditioning

Waste activated sludge was sampled from the wastewater treatment plant of Neili Bread Plant, Presidential Enterprise Co., Taoyuan, Taiwan on July, 2000. A particle sizer (LS230, Coulter, USA) estimated the volume average floc diameters as 73.6 μm . The experimental details of cationic flocculation and freezing/thawing can be found elsewhere and are neglected here for brevity (Chu and Lee, 1999; Chu *et al.*, 1997).

Microscopic techniques

The experimental details of confocal laser scanning microscope (CLSM), fluorescence *in situ* hybridization, and microtome slicing are available in the report of first-year project and are ignored in this section. Details of free settling tests, small angle light scattering (SALS) tests, and the fractal dimensions determined from the two tests are also reported in Wu *et al.* (2002).

Image processing

Sliced images in RGB (red-green-blue) mode are first converted to grayscale images to construct a histogram of pixels versus luminescence intensity by *INSPECTOR* (Matrox, Canada). Our evaluation shows that Otsu's method (Otsu, 1979) yields more stable performance than other histogram-based algorithms and is chosen to obtain the porosity. The $\text{MAX}(\Sigma p_{C,p})$ method, where $p_{C,p}$ represents the convex perimeter of the pores, however, can probe the shapes and spatial distribution of the pores among the biomass granules

Establishing 3D models from CLSM images

Figures 1 display a typical series of CLSM images. Using the Otsu's method, thresholding values of sliced images were determined. **Figure 2** shows the corresponding bilevel images of **Figs. 1**. Noise was removed from the images before bilevel thresholding was performed. The 3D visualization and modeling software, *Amira 3.0* (TGS Inc., USA), was used to reconstruct the thresholded sliced images as isosurfaces (polygonal surface models). The following procedure is employed (TGS, 2002).

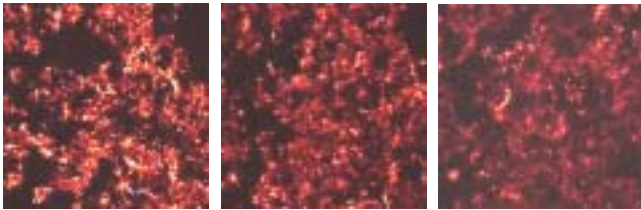


Fig. 1 Example CLSM images in series

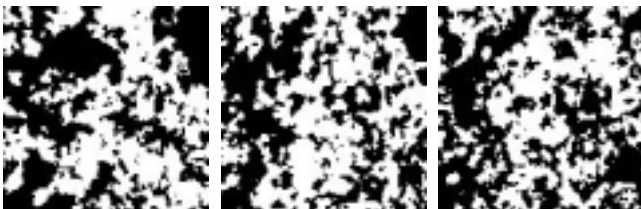


Fig. 2 Bilevel images of **Figs. 2** (by Otsu's method)

(1) The first step is to reduce the resolution of the image and adjust the physical shape of the voxel to almost a cube. The sliced image resolution was reduced from 512*512 to 128*128 so the ratio $X : Y : Z$ of the voxel was about 1 : 1 : 1. The Lanczos filter is used in the resampling.

(2) The second step is to detect the edges in the bilevel images. Boundaries in the binary images are classified according to connectivity and whether they lie within the object or its complement. The connectivity of neighboring pixels in all analyses is set to four for edge detection. The edges in the images are white lines in **Figure 3**.



Fig. 3 Edges on the bilevel images of **Figs. 2**

(3) When the boundaries have been sketched, the isosurfaces can be established to demonstrate the three-dimensional shape of the object. The surface construction algorithm adopted here is the *marching cubes* algorithm for triangulating surfaces (Lorensen and Cline, 1987). Normally, the number of triangular patches on the created isosurfaces is too high to construct volumetric grids. The number of patches should generally be reduced to below 5% of the original number to ensure successful grid generation. **Figure 4a and 4b** presents the original and simplified cases.

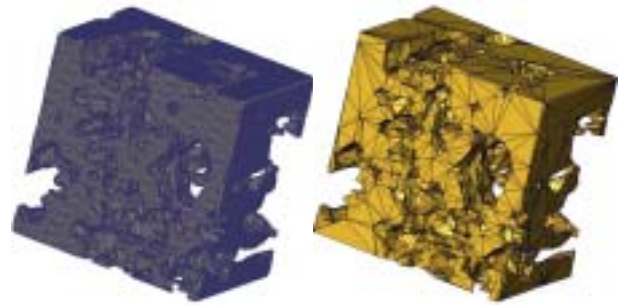


Fig. 4 Polygonal surface model of pores: (a) before simplification (310,534 triangular patches); (b) after simplification (9,000 triangular patches)

IV. Results and Discussion (結果與討論)

The phase contrast microphotographs of original and conditioned sludge flocs can be found elsewhere and are not shown here for brevity (Chen *et al.*, 2001; Chu *et al.*, 2001). For original sludge flocs, filamentous bacteria surrounded a highly porous structure consisting of several microbial aggregates. Polyelectrolyte flocculation significantly increased floc sizes by polymer bridging. Frozen/thawed sludge flocs were also larger and more compact.

The results of SALS tests indicate that floc size increased substantially after flocculation and freezing/thawing. The scattering fractal dimension D_s of both flocculated sludge (1.94) and frozen/thawed sludge

(1.95) decreased. The flocculated sludge had a lower settling fractal dimension D_F (1.30) than the original sludge (1.47), while the frozen/thawed sludge had a higher value (1.55).

Figures 5 to 7 present several examples of typical microtome slices. For original sludge flocs (**Fig. 5**), the microphotograph displayed a cluster of sludges that consist of many flocs with open structures. Pores distributed among the biomass granules were of sizes 20~40 μm . Cationically flocculated sludge flocs had some large pores are larger than 50 μm . Some compact regions were also observed (**Fig. 6**). Frozen/thawed sludge flocs displayed very compact morphology in both microphotographs (**Fig. 7**). The rugged and irregular boundaries of original sludge flocs had become spherical or rectangular pellets after gross migration. The results of geometric parameters are summarized in **Table 1**.



Fig. 5 Sliced images of original sludge: (a) 100X; (b) 400X.

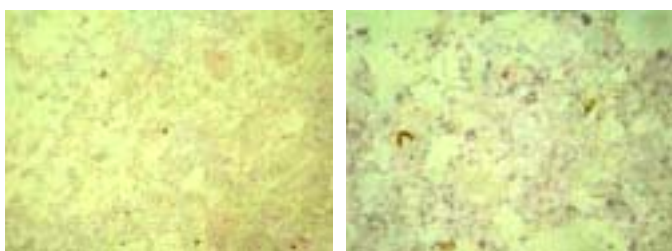


Fig. 6 Sliced images of cationically flocculated sludge: (a) 100X; (b) 400X.



Fig. 7 Sliced images of frozen/thawed sludge: (a) 100X; (b) 400X.

Several typical cases of original, cationically flocculated, and frozen/thawed flocs were considered. **Figures 8 to 10** display CLSM sliced image and three-dimensional views of the biomass portion of the nine selected flocs. The results of geometric parameters are summarized in **Table 1**. Unlike the surface model of reported by Zartarian *et al.* (1997), which only considered external contours, **Figs. 8b to 10b** exhibit the complex

porous configurations of the flocs. Measuring the volume and surface area of the biomass portion can yield other indices such as the fractal dimension. Blob analysis of the CLSM images (512 pixels * 512 pixels) using the $\text{MAX}(\Sigma p_{C,p})$ method also yields the relationship between the area and the perimeters of the biomass granules and the fractal dimension D_B of the boundary. On average, the cationically flocculated sludge flocs had a higher D_B (1.32 ~ 1.36) than the original and frozen/thawed flocs.

Changing the resolution (voxel size) yields different results for the surface area of the sludge flocs, and thus this relationship can help obtain the box-counting fractal dimension $D_{P,3}$. The original sludge flocs had $D_{P,3}$ of about 2.57. Similar to the results for $D_B^{(L)}$, cationic flocculated sludge flocs with more irregular surfaces had the highest $D_{P,3}$ (2.62 ~ 2.70), and frozen/thawed sludge flocs had lower D_P (2.45~2.50) than the original flocs. D_B and $D_{P,3}$ reflect similar morphological information.

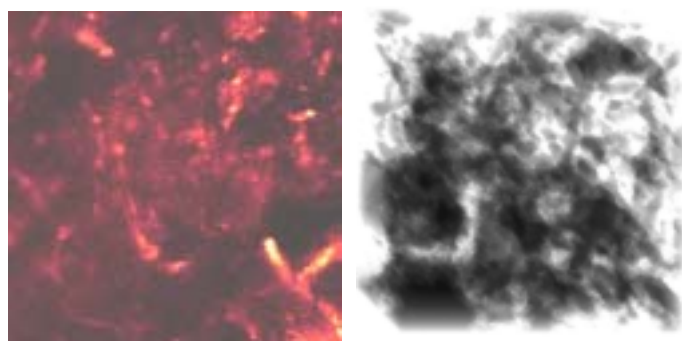


Fig. 8 Original floc: (a) one typical CLSM sliced image; (b) three-dimensional view of floc biomass

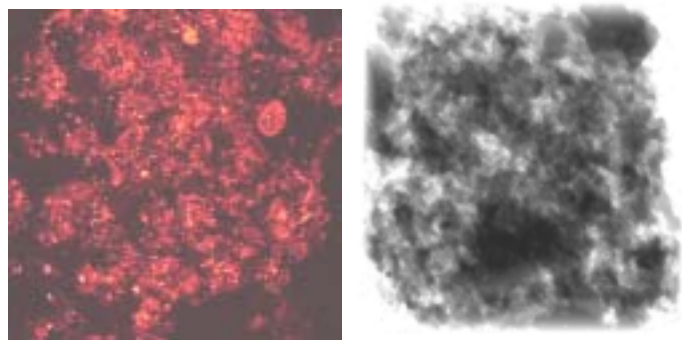


Fig. 9 Flocculated floc: (a) one typical CLSM sliced image; (b) three-dimensional view of floc biomass.

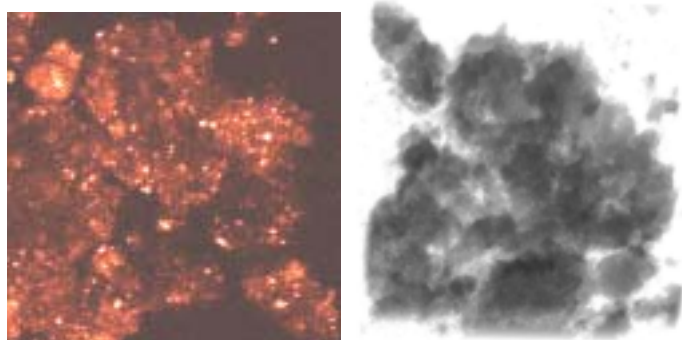


Fig. 10 Frozen/thawed floc: (a) one typical CLSM sliced image; (b) three-dimensional view of floc biomass.

Table 1 The geometric parameters determined from microtome-sliced images and 3D models.

	Size of 3D model ($\mu\text{m} * \mu\text{m} * \mu\text{m}$)	D_F	D_S	$\epsilon_{2D}^{(L)}$	$d_p[4,3]^{(L)}$ (μm)	ϵ_{3D}^{*1}	D_B^{*2}	$D_{P,3}$
Original	93.8*93.8*74.9	1.47	2.18	0.733	23.60	63.6%	1.29	2.57
Flocculated	187.6*187.6*131.8	1.30	1.94	0.684	59.31	53.6%	1.35	2.63
Frozen/thawed	93.8*93.8*51.0	1.55	1.95	0.647	17.54	60.9%	1.27	2.46

*¹ The porosity indicated the volumetric percentage of the empty portion in the cuboids.

*² The area and perimeter were obtained from the image of resolution 512 pixels * 512 pixels.

Possible relationships among D_F , D_S and these parameters, determined by microtome slicing, are considered. Flocs of higher D_F , such as frozen/thawed samples, have a lower $D_{P,3}$ and D_B . However, a simple correlation between porosity and D_F and is hard to derive. $\epsilon_{2D}^{(L)}$ does not singly govern the variation of D_F . A floc with larger pores and lower porosity exhibits lower D_F than another whose size is of the same order of magnitude but with smaller pores and higher porosity. This finding is pertinent to comparisons between the flocculated sludge and frozen/thawed sludge. This result may suggest that free settling behavior might be determined by both the floc size and internal porous configuration, rather than porosity alone.

Notably, D_S was neither correlated with the porosity, nor related to $D_{P,3}$ and D_B . Although the flocculated and frozen/thawed sludge flocs had lower porosity than the original floc, the obtained values of D_S obtained were still significantly lower than that of the original floc. The evidence presented herein could not comprehensively determine the relationship between D_S and other geometric parameters. It implies that the scattering characteristics of these aggregates might not be singly determined by surface morphology.

V. Conclusions (結論)

Based on the proposed image-processing algorithms, a series of sliced images were used to analyze the porous configuration of sludge flocs and reveal the effects of cationic polyelectrolyte flocculation and freezing/thawing. The three-dimensional models of flocs were established using the CLSM series images. Cationic flocculation links the original sludge flocs into a large networked structure with highly non-uniform mass distribution. Both compact biomass granules and large pores are observed. Freezing/thawing markedly compresses the flocs and the porous configuration largely collapses. For flocs with sizes of a particular order of magnitude, the free settling fractal dimension (D_F) correlates with the porosity and pore size of the entire floc matrix. Moreover, flocs of higher D_F , such as frozen/thawed samples, have a lower

$D_{P,3}$ and D_B . The scattering fractal dimension (D_S), however, exhibits no simple relationship with any geometric parameter of the scattering aggregates.

VI. Reference (參考文獻)

- Chen, L. C., Chian, C. Y., Yen, P. S., Chu, C. P. and Lee, D. J. (2001) High-speed freezing of sludge. *Wat. Res.*, **35**(14), 3502-3507.
- Chu, C. P., Lee, D. J., Chang, B. V. and Liao, C. S. (2001) Effect of polyacrylamide on microbial density levels in waste activated sludge. *J. Chem. Tech. Biotechnol.*, **76**(6), 598-602.
- Chu, C. P. and Lee, D. J. (1999) Moisture distributions in sludges: effects of cationic polymer conditioning. *J. Environ. Eng. ASCE*, **125**(4), 340-345.
- Chu, C. P., Feng, W. H., Tsai, Y. H. and Lee, D. J. (1997) Uni-directional freezing of waste activated sludge: The presence of sodium chloride. *Environ. Sci. Tech.*, **31**(5), 1512-1517.
- Jean, D. S., D. J. Lee, and J. C. S. Wu, (1999) Separation of oil from oily sludge by freezing and thawing. *Wat. Res.*, **33**(7), 1756-1759.
- Lorensen, W. E. and Cline, H. E. (1987) Marching cubes: a high resolution 3D surface construction algorithm. *Comput. Graph.*, **21**(4), 163-169.
- Moudgil, B. M. and Shah, B. D. (1986) Selection of flocculants for solid-liquid separation processes, in *Advances in Solid-Liquid Separation*. Ed. by H. S. Muralidhara, Battelle Press, Columbus, Ohio, USA.
- Otsu, N. (1979) A threshold selection method from gray-level histogram. *IEEE Trans. Syst. Man Cybern.*, **9**(1), 62-66.
- TGS (2002) *Amira® 3.0 User's Guide and Reference Manual*. TGS Template Graphics Software, Inc., USA.
- Wu, R. M., Lee, D. J., Waite, T. D. and Guan, J. (2002) Multilevel structure of sludge flocs. *J. Colloid Interf. Sci.*, **252**(2), 383-392.
- Zartarian, F., Mustin, C., Villemin, G., Ait-Ettager, T., Thill, A., Bottero, J. Y., Mallet, J. L. and Snidaro, D. (1997) Three-dimensional modeling of an activated sludge floc. *Langmuir*, **13**(1), 35-40.